A miniaturized, high frequency mechanical scanner for high speed atomic force microscope using suspension on dynamically determined points

Herfst, R.; Dekker, B.; Witvoet, G.; Crowcombe, W.E.; de Lange, D.; Sadeghian Marnani, Hamed

Publication date
2015

Document Version
Final published version

Published in
Review of Scientific Instruments

Citation (APA)
Herfst, R., Dekker, B., Witvoet, G., Crowcombe, W. E., de Lange, D., & Sadeghian Marnani, H. (2015). A miniaturized, high frequency mechanical scanner for high speed atomic force microscope using suspension on dynamically determined points. *Review of Scientific Instruments*, *86*(11), Article 113703.

A miniaturized, high frequency mechanical scanner for high speed atomic force microscope using suspension on dynamically determined points

Rodolf Herfst, Bert Dekker, Gert Witvoet, Will Crowcombe, Dorus de Lange, and Hamed Sadeghian

Citation: Review of Scientific Instruments **86**, 113703 (2015);
View online: https://doi.org/10.1063/1.4935584
View Table of Contents: http://aip.scitation.org/toc/rsi/86/11
Published by the American Institute of Physics

REVIEW OF SCIENTIFIC INSTRUMENTS **86**, 113703 (2015)

A miniaturized, high frequency mechanical scanner for high speed atomic force microscope using suspension on dynamically determined points

Rodolf Herfst,[1] Bert Dekker,[1] Gert Witvoet,[1] Will Crowcombe,[1] Dorus de Lange,[1] and Hamed Sadeghian[1,2,a)]
[1]*Department of Optomechatronics, Netherlands Organization for Applied Scientific Research, TNO, Delft, The Netherlands*
[2]*Department of Precision and Microsystems Engineering, Delft University of Technology, Delft, The Netherlands*

(Received 11 September 2015; accepted 31 October 2015; published online 16 November 2015)

One of the major limitations in the speed of the atomic force microscope (AFM) is the bandwidth of the mechanical scanning stage, especially in the vertical (z) direction. According to the design principles of "light and stiff" and "static determinacy," the bandwidth of the mechanical scanner is limited by the first eigenfrequency of the AFM head in case of tip scanning and by the sample stage in terms of sample scanning. Due to stringent requirements of the system, simply pushing the first eigenfrequency to an ever higher value has reached its limitation. We have developed a miniaturized, high speed AFM scanner in which the dynamics of the z-scanning stage are made insensitive to its surrounding dynamics via suspension of it on specific dynamically determined points. This resulted in a mechanical bandwidth as high as that of the z-actuator (50 kHz) while remaining insensitive to the dynamics of its base and surroundings. The scanner allows a practical z scan range of 2.1 μm. We have demonstrated the applicability of the scanner to the high speed scanning of nanostructures. [http://dx.doi.org/10.1063/1.4935584]

I. INTRODUCTION

The increase of the imaging speed in atomic force microscopy (AFM) is of interest in several practical applications, including wafer inspection in semiconductor applications[1–5] and visualizing dynamic behavior of proteins in a physiological environment.[6,7]

The imaging speed of AFM is determined by the slowest component in the system (cantilever time response,[8,9] bandwidth of cantilever read-out,[10,11] controller bandwidth,[12] and mechanical scanner bandwidth[13–15]). Often the bandwidth of the mechanical scanner in z direction is the major limiting factor in scanning speed.[13,16] This bandwidth is limited by the first eigenfrequency of the z-scanning stage. A piezotube scanner, the most widely used scanner, has a very low resonance frequency, which is typically below 1 KHz.[17] There have been several efforts for increasing the resonance frequency in z direction by employing shear piezoactuators,[18] a counter balance concept,[13] a flexural support,[14] and a micro-electromechanical system (MEMS) based scanning stage.[19] These efforts resulted in high speed z-stages. However, the high speed z-stage is only part of the total AFM head, which also includes its base and surrounding structure and frame. Often the surrounding structure has a very low eigenfrequency, which limits the bandwidth of the z-scanner. If the z-scanner is actuated with a high bandwidth, the dynamic forces of the z-stages also excite the low eigenfrequency of the base, which is seen as parasitic dynamic disturbances on the high speed z-stage. Therefore, one should also make sure that the dynamics of the high speed z-stage is insensitive to its base and surrounding dynamics. We have developed an AFM scan head, in which the high speed z-stage is designed in such a way that at the interface between the z-stage and the surrounding frame, there is no motion while actuating. Therefore, the z-stage does not transfer forces to its surrounding frame and it is thus isolated from parasitic dynamic forces. By doing so, we have achieved very high speed AFM measurements, whilst maintaining the image quality.

This paper is organized as follows: in Section I, the architecture of the AFM head is described. The design of the mechanical high speed z-stage is explained in Section II. Finally, in Section III, the experimental results of the high speed stage are discussed.

II. ARCHITECTURE OF THE AFM HEAD

Recently, we have introduced an architecture for a parallel high throughput AFM,[3,5] which consists of parallel operation of many miniaturized AFM on a large area sample such as semiconductor wafers or optical lithography masks. In order to eliminate the crosstalk, we have opted for a combined tip and sample scanning architecture, where the xy-scanner only moves the sample horizontally and the z-scanner moves the tip in order to follow the topography. This greatly improves the image quality by eliminating scanner induced bow and improving the z-stage response.

The miniaturized, high speed AFM scanner[3] consists of a small unit (scan head) that fits the following components:

- z-stage for high speed positioning of the cantilever with respect to the sample while scanning;

a)Author to whom correspondence should be addressed. Electronic addresses: hamed.sadeghianmarnani@tno.nl and h.sadeghianmarnani@tudelft.nl.

- the optical beam deflection (OBD) system for measuring cantilever's dynamic motion;
- approach motor for positioning and engaging the cantilever towards the sample into the range of the Z-stage;
- optical encoders to determine the location of the cantilever tip with respect to the sample; and
- the surrounding structure and frame to integrate the various modules together.

The scan head can be placed on a table and is mechanically decoupled from the arm that is used to automatically place the head at the desired location.[5] The sample is placed above the scan head onto a scanning stage which performs scanning in the horizontal plane.

Position sensors in the sample stage (capacitive sensors) provide real-time feedback of the stage position. A grid plate on the table provides the location reference for the scanhead. The scanhead incorporates sensors that measure its relative position to the reference lines of the grid plate in X and Y directions and also in rotation around the Z-axis. The scanhead is calibrated to determine the position of its cantilever tip with respect to its base.

Besides the scanhead, the other parts in the measurement loop are the sample, sample stage, sensor mounts, table, and grid plate. This is shown in Figure 1.

Each of these components have to be mechanically and thermally stable enough to guarantee the required total stability of the loop and, therefore, accuracy of the measurement. In the rest of the paper, we will focus on the development of the high speed scan head. To achieve a high measurement bandwidth (target is 50 kHz) and a high accuracy, the scan head has to meet the following requirements:

- the first resonance frequency should be above 50 kHz;
- the frequency response should be as flat as possible from DC up to the start of the first resonance peak;
- the scan head may exhibit no parasitic resonances due to coupling to other components;
- the scan head fits in a volume of $19 \times 45 \times 70\ \text{mm}^3$; and
- should enable at least 2 μm stroke in z-direction.

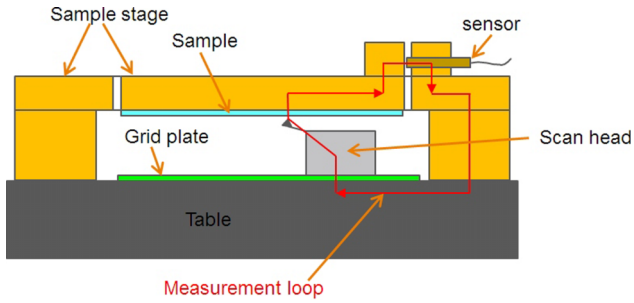

FIG. 1. Schematic overview of the components that constitute the measurement loop.

The configuration of the scan head, shown schematically in Figure 2, is such that the cantilever is the highest point of the scan head. The mechanical z-stage and the complete OBD system are mounted in a guided part of the scan head frame which is moved vertically by the approach motor. On top of the z-stage a dither piezo and cantilever are mounted. The OBD system uses a substantial portion of volume in the design and is folded around the Z-stage to keep the design compact.

To meet the requirements of 50 kHz high bandwidth of the scan head and the flat frequency response, two solutions are available: (a) the entire scan head has an eigenfrequency above 50 kHz or (b) only the mechanical high speed z-stage has an eigenfrequency of 50 kHz while its dynamic response is insensitive to input from the surroundings.

Considering the listed requirements on the rest of the scan head, a 50 kHz eigenfrequency for the entire stage is considered infeasible. This is driven by a higher mass and lower stiffness of the bulk of the scan head compared to the high speed mechanical z-stage. We therefore opted for isolating the dynamics of the high speed z-stage from the rest of the scan head. In case this isolation is not done properly, the very high actuation frequency of the mechanical z-stage can lead to an excitation of the scan head frame. This in turn lowers the measurement bandwidth to the lowest eigenfrequency of the frame which is expected to be in the order of a few kHz (see Figure 3).

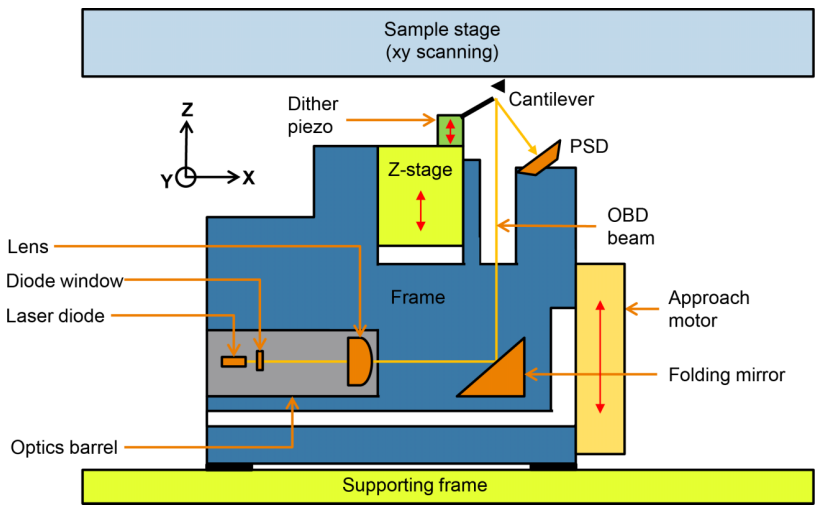

FIG. 2. Schematic representation of the scan head configuration. The approach motor via the flexural guidance (not shown) moves the z-stage, the OBD, and the cantilever towards the sample to engage.

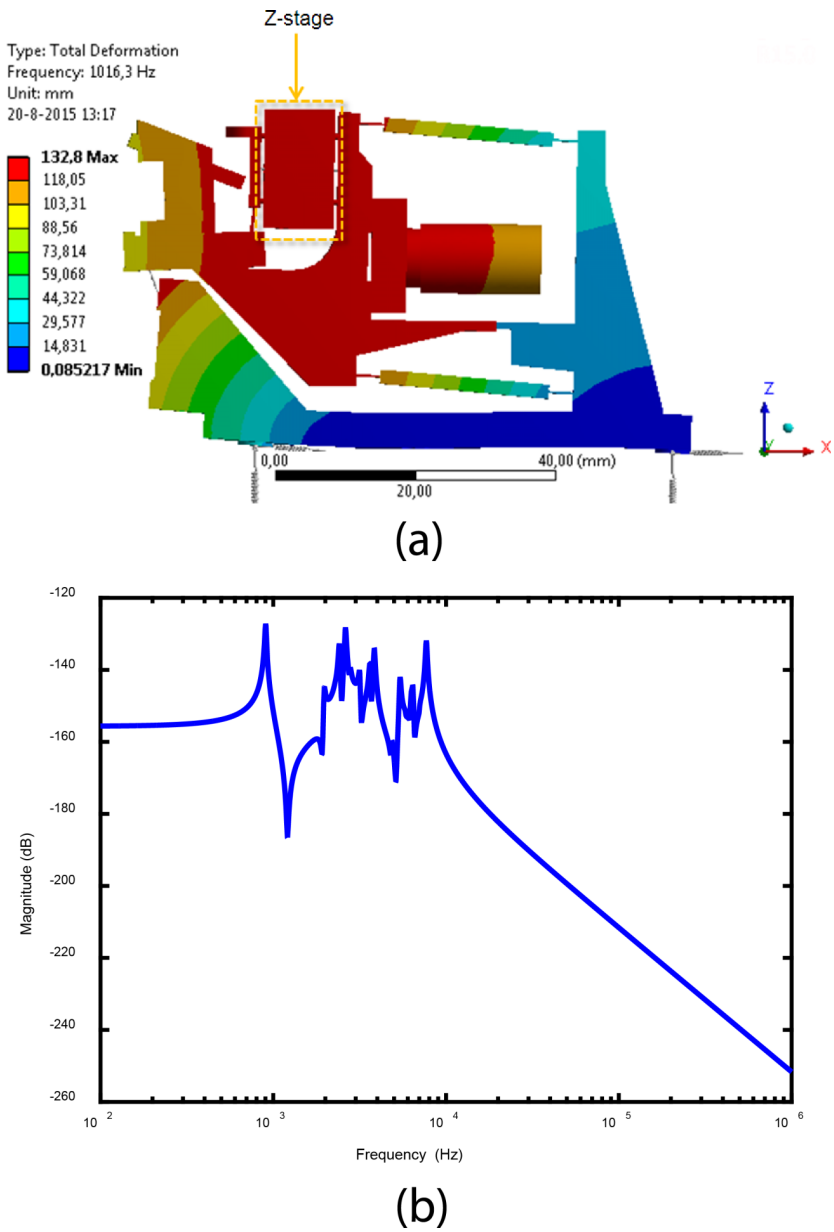

FIG. 3. Dynamics of the AFM scan head. (a) Modal analysis showing lowest mode shape with z-direction component. The eigenfrequency of this mode is about 1 kHz. (b) Frequency response of scan head when actuated.

The statement above has been verified by a modal analysis of the complete scan head which shows that the lowest vertical mode in the scan head with a component in the z-direction is around 1 kHz. In order to eliminate resonances below 50 kHz, an appropriate design strategy has to be used. The used design strategy relies on mounting the mechanical z-stage to the frame in such a way that at the interface, there is no relative motion towards the scan head frame and, thus, the outside world.

III. HIGH SPEED MECHANICAL Z-STAGE

In achieving high eigenfrequencies, both high stiffness and low mass are crucial. For the mechanical z-stage, this requires a high stiffness for the actuation hinges and a low mass for the moving body. Aluminum has been chosen as base material for its availability, easy machining, and also because it matches the material of the scan head frame, reducing effects of thermal mismatch. Since the mechanical z-stage has one translational degree of freedom, a monolithic structure can be achieved by electrical discharge machining (EDM). To maximize the stiffness while maintaining a low mass, an aluminum with high Young's modulus was used. Further increase of the stiffness has been achieved by using multiple flexures in parallel, as depicted in Figure 4. Moreover, reducing the gap between each set of flexures and using 4 sets increased the torsional stiffness of the z-stage.

The high speed displacement of the piezoactuator causes a large inertial force on the frame of the scan head. The induced vibrations of the frame and its surrounding mechanisms in turn cause vibrations of the actuator itself. In order to partially cancel these parasitic forces a counter balanced configuration is implemented.[13,16,20] Here, two identical piezoactuators work against each other (shown in Figure 4). Inertial forces resulting from the movement of the top side of the z-stage are

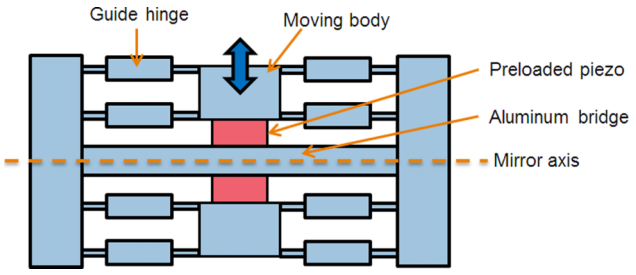

FIG. 4. Schematic layout of the mechanical z-stage. Stacked multiple flexures in parallel were used to (1) achieve high stiffness and (2) increase the torsional stiffness.

countered by the simultaneous displacement of the bottom side in the opposite direction so that its center of mass remains unchanged.[20]

A small aluminum bridge was maintained between the two piezoactuators to connect them to the z-stage frame, preventing a rigid body motion of the coupled actuators.

Finite element analysis of the structure as shown in Figure 5 indicates that the stresses in the flexure remain shy of the 100 MPa fatigue limit of the material. The design allows for the intended piezostroke of 2 μm including an additional 7 μm stroke for prestressing the piezos.

The cantilever is mounted in a small holder on top of the dither piezo which is placed on top of the z-stage. The mass of these components disturbs the balanced situation that was achieved by the symmetry in the z-stage in x-, y-, and z-directions; not only along the z-axis but also around the y-axis symmetry (and balance) is lost because the cantilever holder is mounted in an off-center position. Hence, to eliminate the effect of these small asymmetries on the overall dynamics, three dummy dither elements have been added to the z-stage.

Also the placement accuracy of the piezoactuators with respect to each other and the symmetry planes of the z-stage are important to ensure a pure vertical motion while minimizing disturbances around or along other axes.

The piezoactuators are mounted with a compressive preload which reduces creep and also protects the piezo from tensile induced cracks due to high accelerations. Cavities are machined into the moving body of the z-stage for mass reduction and to provide handling points for pulling apart the mating faces when the piezoactuators are mounted.

Free body modal analysis of the z-stage has been performed to investigate the mode shapes and to determine the most suitable locations for interfacing the z-stage to the surrounding frame. The 5th mode shape at ~50 kHz is that of the actuation motion of the z-stage. The first 4 mode shapes have been constrained by the surrounding frame.

As it can be seen in Figures 6 and 7, four areas can be identified where there is very little translational movement of the frame when this particular mode is excited. This means, if the mechanical z-stage is clamped to the rest of scan head frame in these four areas, there will be very little relative motion between the z-stage and the rest of the frame, thus the dynamics response of the high speed z-stage is not disturbed by the dynamics of the surrounding structure at that specific eigenfrequency. In order to minimize coupling of the motion with the frame, further analyses were performed to locate the exact points within these areas where the deformation is zero. These four points are so-called *stationary points*, as there are only rotations and no translations at these points exist.

As a starting point for determining the exact positions of the stationary points, a free-body static analysis with a unit force on the piezosurfaces was performed (as shown in Figure 7). For each area of interest, the y- and z-displacements

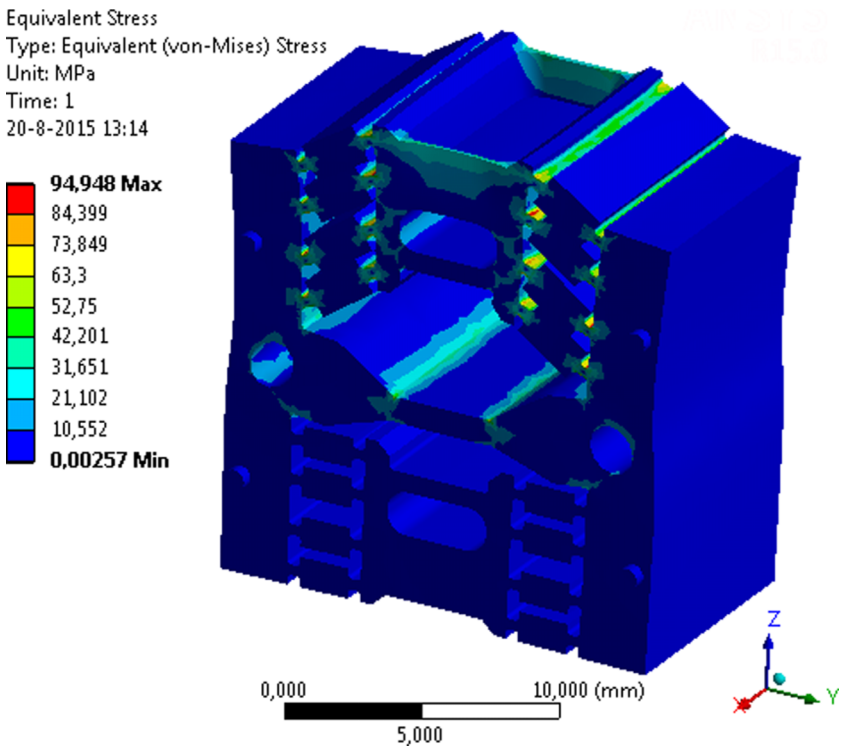

FIG. 5. Finite element stress analysis of the z-stage at maximum stage deflection.

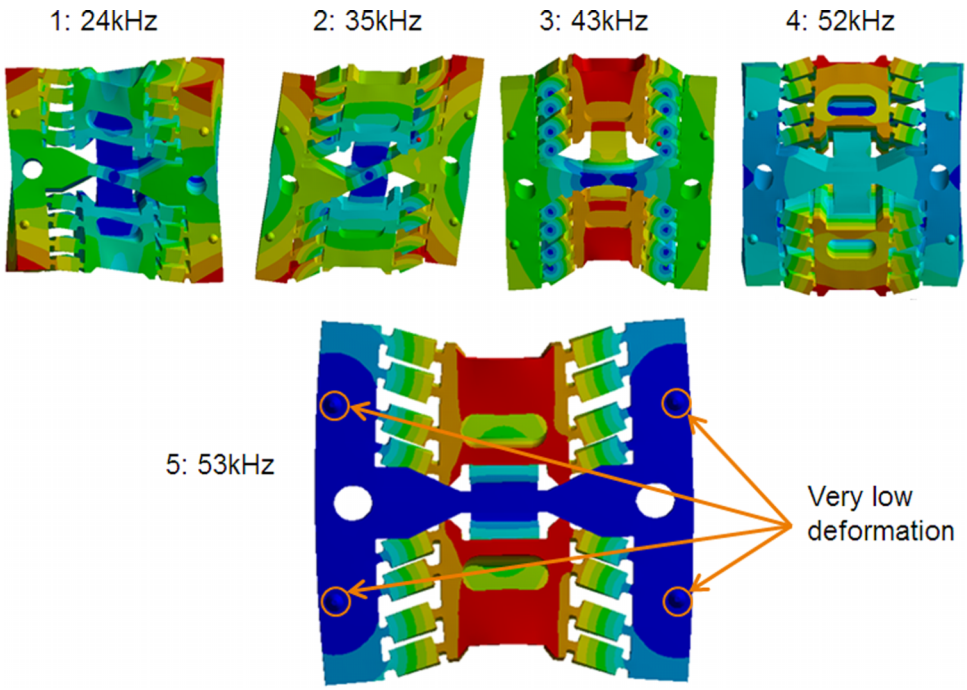

FIG. 6. The first five mode shapes of the z-stage, with mode five as the actuation mode.

of the nodes were exported and sorted by displacement size. By plotting a selection of these lowest displacements, a line graph is obtained for each axis, showing the line location within the area of interest where the deformation of that particular direction is zero. When plotted in one graph, the lowest y- and z-displacement lines intersect at the point of lowest deformation (Figure 7, right figure). This provided the initial location of the four points.

For the complete scan head assembly, in the range up to 50 kHz, two eigenmodes containing motions in the z-direction have been identified that can be excited by the z-stage, the first one at 1 kHz and the second one at 2 kHz. In a subsequent dynamic analysis, the positions of the stationary points have been further optimized for lowest gain fluctuation at these two modes by creating a fine mesh grid around the previously found point locations and calculating the gain amplitude belonging to each of the grid locations. This showed that a small shift from the initial point locations was needed to further improve the performance, resulting in a <0.02 dB transfer amplitude for the 1 kHz and 2 kHz eigenmodes.

It is noteworthy to mention that these points also need to be fixed at the back of the z-stage to maintain symmetry, which results in a mechanical interface on both sides of the stage.

In practice, the z-stage has been given four small protrusions on both front and back side. The protrusions at the back side of the stage fit into four precision machined holes of the scan head frame. With the rear interface, all the degrees of freedom of the z-stage frame were fixed. To achieve symmetry in vertical stiffness, a separate bracket interfaces with the front protrusions. Figure 8 shows the bracket has various features to prevent a statically overdetermined fixation of the z-stage. Vertically machined V-grooves interface with the front protrusions of the z-stage, providing translational freedom along the z-axis and also for rotation around the x-axis. A flexure element at the top center of the bracket provides rotational freedom around the y-axis while two flexures at the bottom provide rotational freedom around the z-axis. The two bottom flexures also give the bracket translational freedom along the x-axis. Translation along the y-axis is provided by shifting the bracket a little prior to tightening the bolts. Two bolt holes at

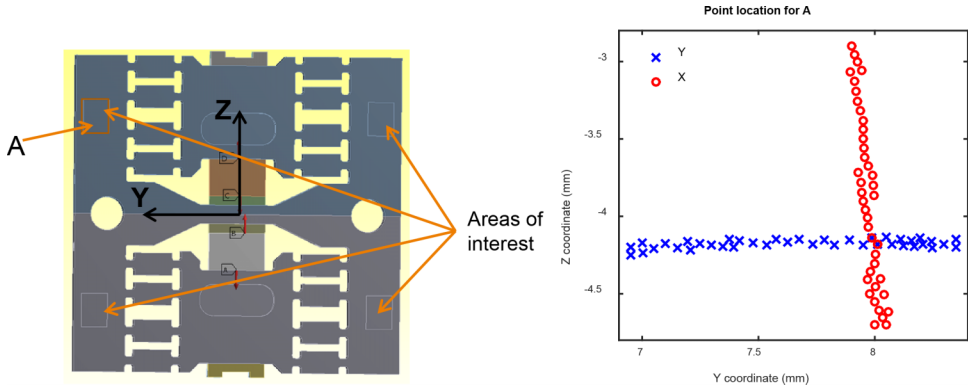

FIG. 7. Left: areas of interest for optimization. Right: statically optimized point location for area A.

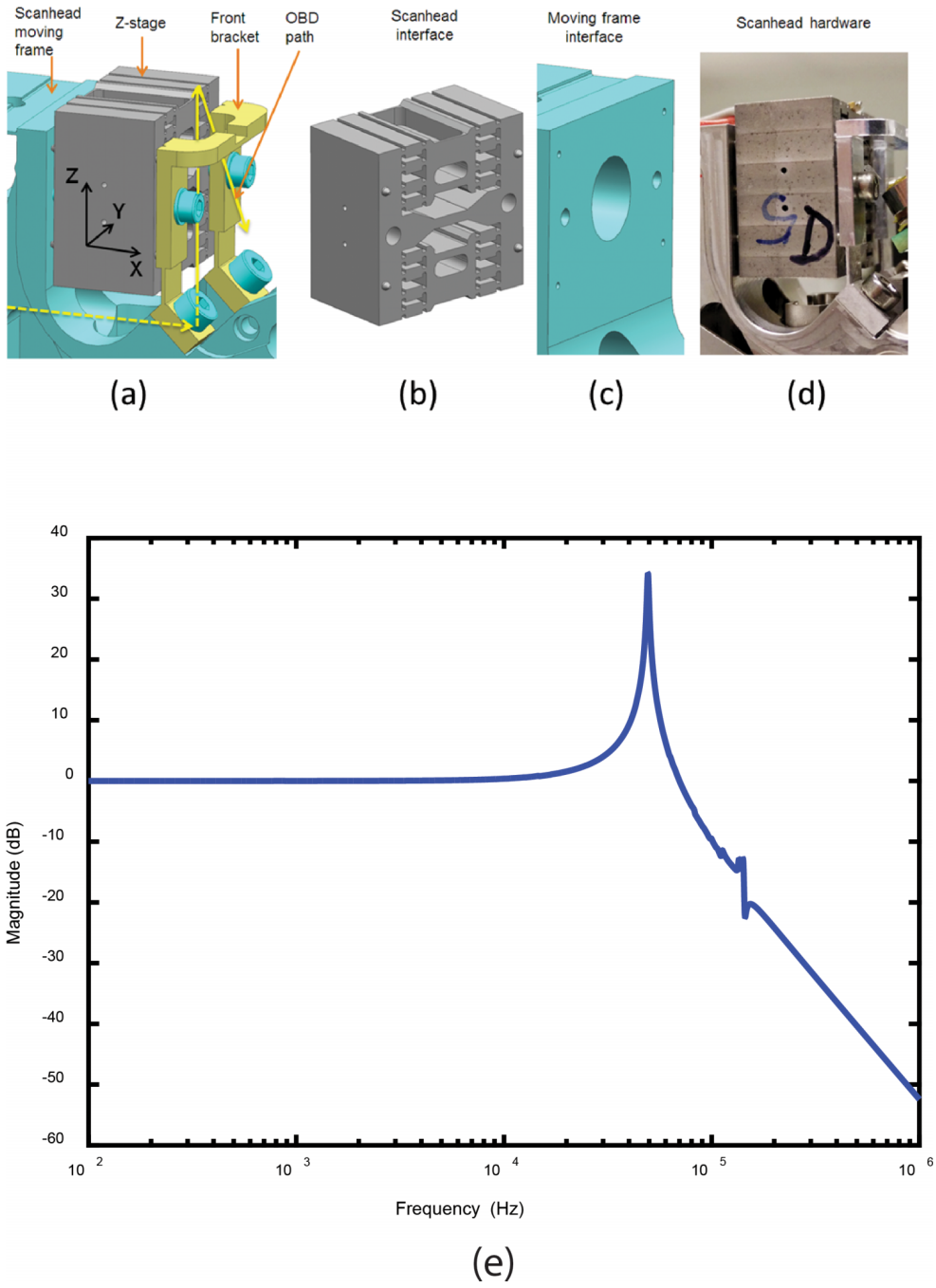

FIG. 8. (a) Integrated z-stage. (b) Z-stage interface protrusions. (c) Interface of scan head frame. (d) Realized hardware. (e) The frequency spectra after balancing the high speed z-stage.

the center of the z-stage provide the means of preloading the z-stage onto its stationary point interfaces by using the elasticity of the front bracket as a spring. The bracket is partially split and has a hoof-shaped top area to accommodate the OBD beam.

IV. EXPERIMENTAL RESULTS

For the experimental verification of the z-stage and scan head concept, four scan heads (including z-stages) were manufactured. To achieve the desired performance, special attention was put into fabrication and assembly of the z-stages. This consisted of fabricating the z-stage using wire-erosion and precise milling, creation of shims to ensure an equal amount of pre-stress on each of the two piezo-actuators, and carefully aligning and centering them to minimize imbalances. After the dither piezo with cantilever holder is mounted on top of the z-stage, the frequency response of the z-stage is fine-tuned with counter balance mass underneath the z-stage.

After insertion of the piezo-actuator into the z-stage, we first determined the performance without the mass of the dither piezo and cantilever holder altering its behavior. A single-point Polytec laser vibrometer was used to determine displacement and velocity in the z-direction while applying various signals to the piezoactuators. By applying a 200 Hz, 150 V peak-to-peak sine wave the maximum stroke of the four tested

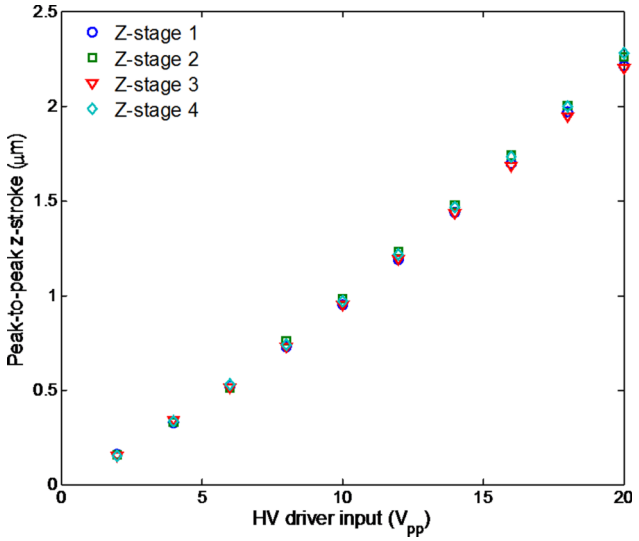

FIG. 9. Stroke of the four z-stages as function of input voltage swing. Maximum peak-to-peak stroke was 2.24 ± 0.04 μm.

z-stages was determined to be 2.2 μm. The relation between input voltage swing and peak-to-peak stroke is shown in Figure 9.

To obtain the frequency response of the 4 z-stages, a 3.0 V peak-to-peak sine sweep from 2.5 to 100 kHz was used. The z-stage was not yet mounted in the scan head, but instead mounted on a test jig containing the same four stationary points as the scan head. The result of this is shown in Figure 10. At low frequency, there is an almost completely flat response. Above 20 kHz, the effect of the first resonance starts to become visible. The first resonance frequency was between 51 and 54 kHz for all four z-stages, proving the reproducibility of our manufacturing and assembly methodology.

Next, the weighed stack of dither piezo and cantilever holder (0.104 g total) was mounted on top of the z-stage. Three counterbalance masses were produced (0.094 g, 0.104 g, and 0.114 g) and temporarily attached opposite to the cantilever holder. We then checked which of the three masses resulted in the best balance. The result of this is shown for one of the z-stages in Figure 11. As expected, the imbalance introduced by dither piezo and cantilever holder leads to significant deterioration of the frequency response with a large resonance/anti-resonance pair at 36.5 kHz. Matching it with a counterbalance of equal mass results in the best overall frequency response: flat for low frequency and a single symmetric resonance peak. Note that the quality factor is a little bit lower than without loading. We suspect this is due to slight damping effects in the thin layer of wax that was used to temporarily fix the counter balance mass to the z-stages.

After balancing the four z-stages, each had their first resonance between 46.5 kHz and 47.5 kHz. This is a few kHz lower than the unloaded z-stages due to the added mass. The tight spread in resonance frequency proves the reproducibility of our assembly and balancing strategy.

To check whether the use of balancing and the carefully chosen stationary points indeed results in a low mechanical coupling between z-stage and scan head frame, we mounted the z-stages in the scan heads and measured the frequency response of the z-actuator in the final configuration.

Figure 12 shows a more detailed frequency response measured from 200 Hz upwards to also rule out resonances below 1 kHz. Here, we can see that the frequency response is very flat between 200 Hz and 10 kHz, it stays within a band of ±0.3 dB, i.e., 3.5% variation of position amplitude. From this can be concluded that no scan head modes are excited, i.e., the stationary points result in a good decoupling between the z-stage and the scan head. Note that for practical reasons (signal to noise ratio (SNR) and dynamic range of our measurement system), this result is a composite of two sweeps with an amplitude of 10 V peak-to-peak and 3.0 V peak-to-peak, respectively.

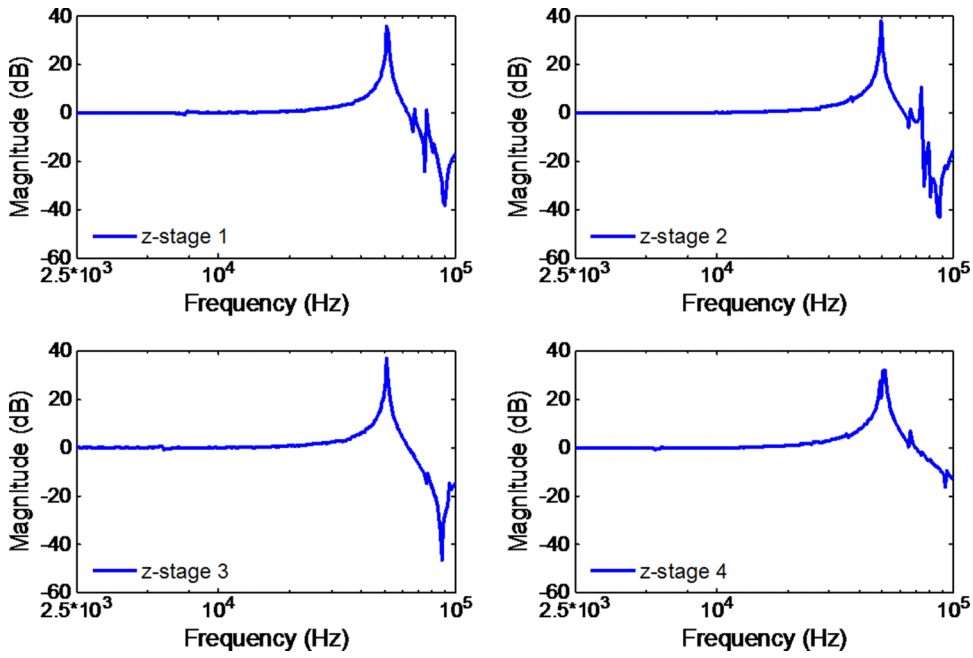

FIG. 10. Vibration amplitude as function of frequency as result of a 3.0 V (peak-to-peak) swept sine signal. Z-stages were mounted in the testing tool.

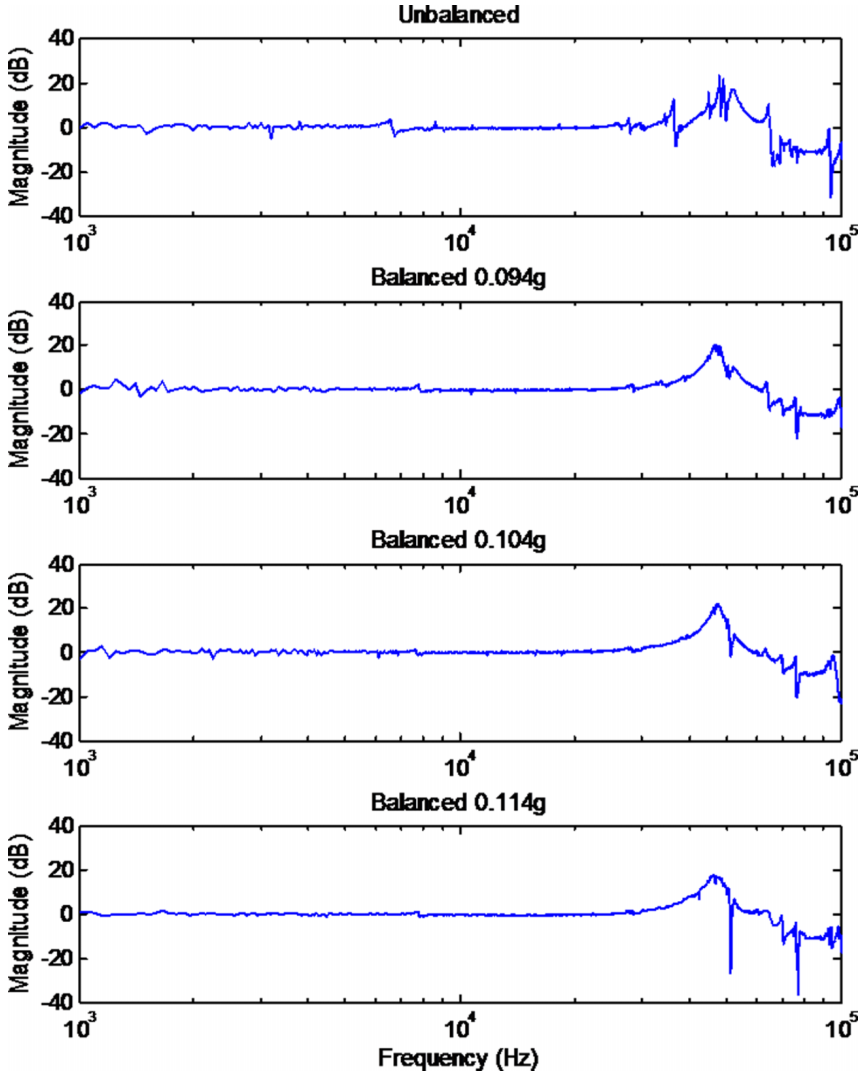

FIG. 11. Effect of using a counterbalance to compensate for the asymmetric load that is introduced when a dither piezo and cantilever holder (total weight: 0.104 g) are mounted to the z-stage. Frequency response obtained by applying a 1–100 kHz, 2.5 V rms sine sweep and measuring the amplitude with a laser vibrometer. Z-stages were mounted in the testing tool.

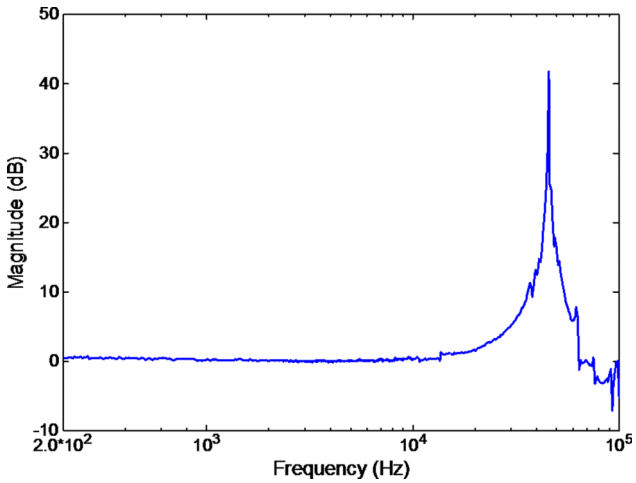

FIG. 12. Frequency response of a z-stage mounted in the scan head measured from 200 Hz up to 100 kHz. To increase signal/noise at low frequencies, the applied amplitude was 10.0 V peak-to-peak from 200 Hz to 10 kHz. Above this, it was reduced to 3.0 V peak-to-peak to keep the large signal swings at the resonance peak within the limits of the measurement system.

After connecting the scan head to the arm that is used to automatically place the head at the desired location,[5] we used a small XY stage and an AFM controller to scan a test sample. For this, we used a NanoWorld Arrow UHF probe with a resonance frequency of 1.19 MHz at two different scan rates of 20 Hz and 30 Hz, respectively. The result of this is shown in Figure 13. Here, we see that despite the high line rate and high-frequency content of the structure the topography can be accurately followed. When comparing the cross section of Figures 13(a) and 13(b) (i.e., the blue and green lines in 13(e)), we see that at 30 Hz there is a bit more overshoot present and the features are slightly rounded off, but overall still very similar to scanning at 20 Hz. The error signal exhibits more contrast at 30 lines/s as well, also indicating a slight reduction of how well the samples features can be followed by the system. While the bandwidth of the system enables measurements at high speed, the 2.2 μm stroke of the z-stage ensures the system still performs well when the tested structures have large long-rang slopes (the measurements shown in Figure 13 were corrected for slope and offset).

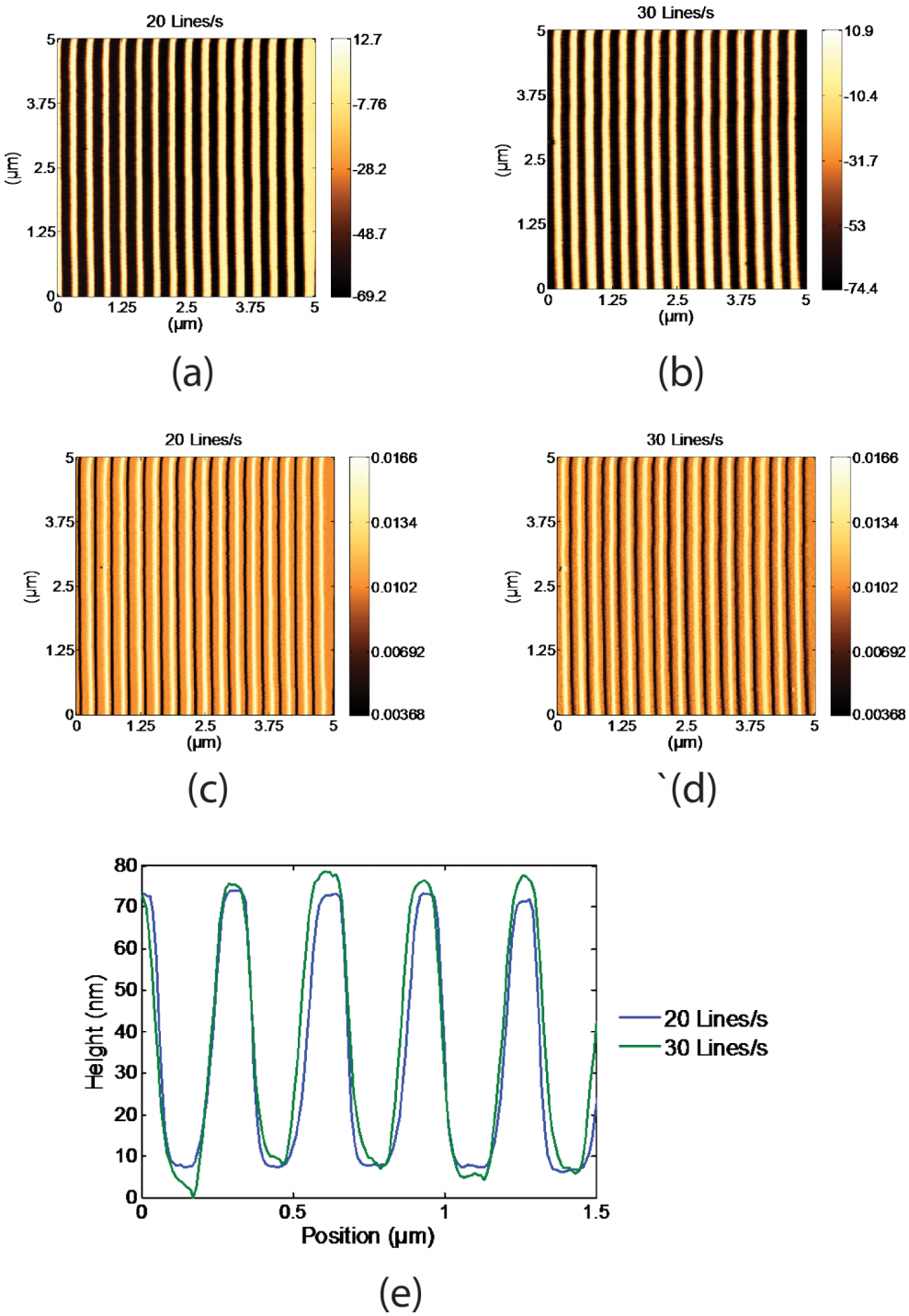

FIG. 13. AFM scan of a 320 nm pitch line sample using a z-stage as mentioned in this work at two different speeds (20 and 30 lines/s, respectively, corresponding to 0.1 and 0.15 mm/s). Resolution: 512×512 pixels, 5×5 μm. Measurements were obtained using a NanoWorld Arrow UHF cantilever at 1.19 MHz. (a) Topography at 20 lines/s (color scale in nm). (b) Topography at 30 lines/s (color scale in nm). (c) Error signal at 20 line/s (color scale in V). (d) Error signal at 20 lines/s (color scale in V). (e) Cross section of the measured topography.

V. CONCLUSIONS

High throughput atomic force microscopy requires a system capable of fast scanning. This puts strict requirements on the stability of the metrology frame as well as the bandwidth of the actuators and sensors constituting the system. If large samples such as wafers are to be measured, high bandwidth z-movement of the sample is not a viable option, so that a high-speed z-actuator for the AFM cantilever is required.

We designed and realized such a high-speed z-stage. By employing a balanced and symmetric design, it has enough stroke (2.2 μm) for a large range of applications with a bandwidth of approximately 50 kHz. In order to prevent excitation of the low frequency support, we mechanically decoupled the high-speed z-stage from the rest of the scan head by the use of stationary points. This z-stage and stationary point concept was used in an actual working high-speed AFM. This high speed scan head is now being

used in a parallel AFM architecture for inspection and metrology of large samples such as semiconductor wafers and masks.

ACKNOWLEDGMENTS

This work was supported by Netherlands Organization for Applied scientific Research, TNO, Early Research Program 3D Nanomanufacturing Instruments. The authors acknowledge Mr. Hans van den Berg from TNO, for his help in fabricating the samples and Mr. Roy Bijster for helpful suggestions.

[1]Y. Martin and H. K. Wickramasinghe, "Toward accurate metrology with scanning force microscopes," J. Vac. Sci. Technol., B **13**, 2335 (1995).
[2]G. Borionettia, A. Bazzalia, and R. Orizioa, "Atomic force microscopy: A powerful tool for surface defect and morphology inspection in semiconductor industry," Eur. Phys. J.: Appl. Phys. **27**(1-3), 101–106 (2004).
[3]H. Sadeghian, N. Koster, and T. v. d. Dool, "Introduction of a high throughput SPM for defect inspection and process control," Proc. SPIE 8681 868127 (2013).
[4]H. Sadeghian, T. C. v. d. Dool, W. E. Crowcombe, R. W. Herfst, J. Winters, G. F. I. J. Kramer, and N. B. Koster, "Parallel, miniaturized scanning probe microscope for defect inspection and review," Proc. SPIE **9050**, 90501B (2014).
[5]H. Sadeghian, B. Dekker, R. Herfst, J. Winters, A. Eigenraam, R. Rijnbeek, and N. Nulkes, "Demonstration of parallel scanning probe microscope for high throughput metrology and inspection," Proc. SPIE **9424**, 94240O (2015).
[6]T. Andoa, T. Uchihashi, and T. Fukuma, "High-speed atomic force microscopy for nano-visualization of dynamic biomolecular processes," Prog. Surf. Sci. **83**(7-9), 337–437 (2008).
[7]M. Imamura, T. Uchihashi, T. Ando, A. Leifert, U. Simon, A. D. Malay, and A. J. G. Heddle, "Probing structural dynamics of an artificial protein cage using high-speed atomic force microscopy," Nano Lett. **15**(2), 1331–1335 (2015).
[8]A. P. Nievergelt, B. W. Erickson, N. Hosseini, J. D. Adams, and G. E. Fantner, "Studying biological membranes with extended range high-speed atomic force microscopy," Sci. Rep. **5**, 11987 (2015).
[9]R. J. F. Bijster, J. d. Vreugd, and A. H. Sadeghian, "Phase lag deduced information in photo-thermal actuation for nano-mechanical systems characterization," Appl. Phys. Lett. **105**, 073109 (2014).
[10]R. Enning, D. Ziegler, A. Nievergelt, R. Friedlos, K. Venkataramani, and A. Stemmer, "A high frequency sensor for optical beam deflection atomic force microscopy," Rev. Sci. Instrum. **82**(4), 043705 (2011).
[11]R. Herfst, W. Klop, M. Eschen, T. v. d. Dool, N. Koster, and H. Sadeghian, "Systematic characterization of optical beam deflection measurement system for micro and nanomechanical systems," Measurement **56**, 104–116 (2014).
[12]G. Schitter, P. Menold, H. Knapp, F. Allgöwer, and A. Stemmer, "High performance feedback for fast scanning atomic force microscopes," Rev. Sci. Instrum. **72**(8), 3320–3327 (2001).
[13]T. Fukuma, Y. Okazaki, N. Kodera, T. Uchihashi, and T. Ando, "High resonance frequency force microscope scanner using inertia balance support," Appl. Phys. Lett. **92**, 243119 (2008).
[14]B. J. Kenton and K. K. Leang, "Design and control of a three-axis serial-kinematic high-bandwidth nanopositioner," IEEE/ASME Trans. Mechatronics **17**(2), 356–369 (2011).
[15]Y. K. Yong, S. O. R. Moheimani, B. J. Kenton, and K. K. Leang, "High-speed flexure-guided nanopositioning: Mechanical design and control issues," Rev. Sci. Instrum. **83**, 121101 (2012).
[16]T. Ando, T. Uchihashi, and N. Kodera, "High-speed atomic force microscopy," Jpn. J. Appl. Phys., Part 1 **51**, 08KA02 (2012).
[17]G. Schitter and A. Stemmer, "Identification and open-loop tracking control of a piezoelectric tube scanner for high-speed scanning-probe microscopy," IEEE Trans. Control Syst. Technol. **12**(3), 449–454 (2004).
[18]M. J. Rost, P. S. L. Crama, E. v. Tol, G. B. E. M. v. Velzen-Williams, C. F. Overgauw, H. t. Horst, H. Dekker, B. Okhuijsen, M. Seynen, A. Vijftigschild, P. Han, A. J. Katan, K. Schoots, R. Schumm, W. v. Loo, T. H. Oosterkamp, and J. W. M. Frenken, "Scanning probe microscopes go video rate and beyond," Rev. Sci. Instrum. **76**, 053710 (2005).
[19]F. Tabak, E. C. M. Disseldorp, G. H. Wortel, A. J. Katan, M. B. S. Hesselberth, T. H. Oosterkamp, J. Frenken, and W. Spengen, "MEMS-based fast scanning probe microscopes," Ultramicroscopy **110**(6), 599–604 (2010).
[20]I. S. Bozchalooi, K. Youcef-Toumi, D. J. Burns, and A. G. E. Fantner, "Compensator design for improved counterbalancing in high speed atomic force microscopy," Rev. Sci. Instrum. **82**(11), 113712 (2011).